



"Compact and Efficient Encryption/Decryption Module for FPGA Implementation of the AES Rijndael Very Well Suited for Small Embedded Applications"

Rouvroy, Gaël ; Standaert, François-Xavier ; Quisquater, Jean-Jacques ; Legat, Jean-Didier

Abstract

Hardware implementations of the Advanced Encryption Standard (AES) Rijndael algorithm have recently been the object of an intensive evaluation. Several papers describe efficient architectures for ASICs (ASIC: Application Specific Integrated Circuit) and FPGAs (FPGA: Field Programmable Gate Array). In this context, the highest effort was devoted to high throughput (up to 20 Gbps) encryptiononly designs, fewer works studied low area encryptiononly architectures and only a few papers have investigated low area encryption/decryption structures. However, in practice, only a few applications need throughput up to 20 Gbps while flexible and low cost encryption/decryption solutions are needed to protect sensible data, especially for embedded hardware applications. This paper proposes an efficient solution to combine Rijndael encryption and decryption in one FPGA design, with a strong focus on low area constraints. The proposed design fits into the smallest Xilinx FPGAs (Xilinx Spartan-3 XC3S...

Document type : *Communication à un colloque (Conference Paper)*

Référence bibliographique

Rouvroy, Gaël ; Standaert, François-Xavier ; Quisquater, Jean-Jacques ; Legat, Jean-Didier. *Compact and Efficient Encryption/Decryption Module for FPGA Implementation of the AES Rijndael Very Well Suited for Small Embedded Applications*. Proceedings of ITCC 2004 (Las Vegas, USA, April 2004).

Compact and Efficient Encryption/Decryption Module for FPGA Implementation of the AES Rijndael Very Well Suited for Small Embedded Applications

Gaël Rouvroy, François-Xavier Standaert,
Jean-Jacques Quisquater and Jean-Didier Legat

*UCL Crypto Group
Laboratoire de Microélectronique
Université catholique de Louvain
Place du Levant, 3, B-1348 Louvain-la-Neuve, Belgium
rouvroy,standaert,quisquater,legat@dice.ucl.ac.be*

Abstract

Hardware implementations of the Advanced Encryption Standard (AES) Rijndael algorithm have recently been the object of an intensive evaluation. Several papers describe efficient architectures for ASICs¹ and FPGAs². In this context, the highest effort was devoted to high throughput (up to 20 Gbps) encryption-only designs, fewer works studied low area encryption-only architectures and only a few papers have investigated low area encryption/decryption structures. However, in practice, only a few applications need throughput up to 20 Gbps while flexible and low cost encryption/decryption solutions are needed to protect sensible data, especially for embedded hardware applications. This paper proposes an efficient solution to combine Rijndael encryption and decryption in one FPGA design, with a strong focus on low area constraints. The proposed design fits into the smallest Xilinx FPGAs³, deals with data streams of 208 Mbps, uses 163 slices and 3 RAM blocks and improves by 68% the best-known similar designs in terms of ratio Throughput/Area. We also propose implementations in other FPGA Families (Xilinx Virtex-II) and comparisons with similar DES, triple-DES and AES implementations.

Keywords: Cryptography, AES, DES, FPGA, compact encryption/decryption implementation, embedded

systems.

1. Introduction

In October 2000, NIST (National Institute of Standards and Technology) selected Rijndael [4] as the new Advanced Encryption Standard (AES), in order to replace the old Data Encryption Standard (DES). The selection process included performance evaluation on both software and hardware platforms and many hardware architectures were proposed. However, most of these architectures simply transcript the algorithm into hardware designs, without relevant optimizations and tradeoffs. Moreover, the throughput and area constraints considered are often unrealistic as shown by the recently published results.

First, many very high-speed (≥ 10 Gbps) cipher hardware implementations have been published in the literature. These designs consists of FPGA implementations of a complete unrolled and pipelined cipher. The best such DES implementation is an encryptor/decryptor based on a new mathematical description. It can achieve data rates of 21.3 Gbps in Virtex-II FPGAs [15]. The encryption/decryption mode can be changed on a cycle-by-cycle basis with no dead cycles. For the AES, the best similar RAM-based solution unrolls the 10 cipher rounds and pipelines them in an encryption-only process. This implementation in a Virtex-E FPGA produces a throughput of 11.8 Gbps [17, 18] and allows the key to be changed at every cycle. This DES implementation reaches higher throughput than the corresponding AES implementation.

¹ASIC: Application Specific Integrated Circuit.

²FPGA: Field Programmable Gate Array.

³Xilinx Spartan-3 XC3S50.

However, these speed efficient designs are not always relevant solutions. Many applications require smaller throughput (wireless communication, digital cinema, pay TV, ...). Sequential designs based on a 1-round loop may be judicious and attractive in terms of hardware cost for many embedded applications. Several such implementations have been published in the literature. For DES and triple-DES designs, the most efficient solution [16] encrypts/decrypts in 18 cycles with a fresh key. For AES, the best design based on 1-round loop [17, 18] produces a data rate of 1450 Mbps (Virtex-E) using 542 slices and 10 RAM blocks, but it does not support the decryption mode. Another efficient circuit [20] proposes a compact architecture that combines encryption and decryption. It executes 1 round in four cycles and produces a throughput of 166 Mbps (Spartan-II) using 222 slices and 3 RAM blocks.

The design proposed in this paper is also based on a quarter of round loop implementation and improves by 68% (in term of ratio $Throughput/Area$) the design detailed in [20]. We investigate a good combination of encryption/decryption and place a strong focus on a very low area constraints. The resulting design fits in the smallest Xilinx devices (e.g. the Spartan-3 XC3S50 and Virtex-II XC2V40), achieves a data stream of 208 Mbps (using 163 slices, 3 RAM blocks) and 358 Mbps (using 146 slices, 3 RAM blocks), respectively in Spartan-3 and Virtex-II devices. It attempts to create a bridge between throughput and cost requirements for embedded applications.

The paper is organized as follows: section 2 describes the smallest Spartan-3 and Virtex-II devices; the mathematical description of Rijndael is in section 3; section 4 describes our sequential AES encryptor/decryptor; finally, section 5 concludes this paper.

2. Spartan-3 and CLB description: the XC3S50 component

The Spartan-3 configurable logic blocks (CLBs) are organized in an array and are used to build combinatorial and synchronous logic designs. Each CLB element is tied to a switch matrix to access the general routing matrix, as shown in Figure 1. A CLB element includes 4 similar slices, with fast local feedback within the CLB. The four slices are split into two columns of two slices with two independent carry logic chains and one common shift chain.

Each slice includes two 4-input function generators, carry logic, arithmetic logic gates, multiplexers and two storage elements. As shown in Figure 2, each 4-input function generator is programmable as

a 4-input LUT, 16 bits of distributed SelectRAM memory, or a 16-bit variable-tap shift register element. The output from the function generator in each slice drives both the slice output and the D input of the storage element.

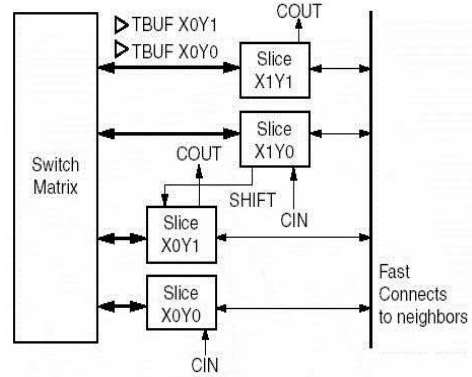


Figure 1. The Spartan-3 CLB.

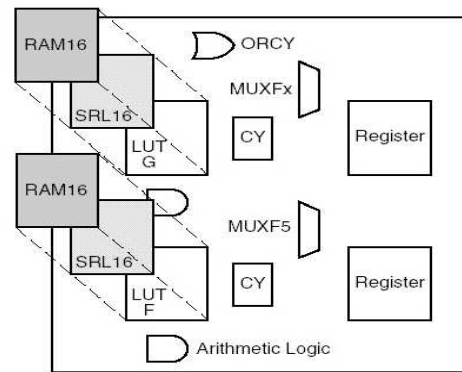


Figure 2. The Spartan-3 slice.

A specific feature of the slice is the 16-bit shift register configuration. The write operation is synchronous with a clock input and an optional clock enable. A dynamic read access is performed through the 4-bit address bus.

Spartan-3 devices also incorporate 18-Kbit RAM blocks. These ones complement the distributed SelectRAM resources provided by the CLBs. Each RAM block is an 18-Kbit true dual-port RAM with two independently clocked and independently controlled synchronous ports that access a common storage area. Both ports are functionally identical.

Virtex-II devices exploit the same architecture as Spartan-3.

The XC3S50 and XC2V40 components are, respectively, the smallest Spartan-3 and Virtex-II compo-

nents. Table 1 illustrates the logic resources available in both components.

Component	XC3S50	XC2V40
CLB array: row \times col.	16×12	8×8
Number of slices	768	256
Number of flip-flops	1,536	512
Number of LUTs	1,536	512
Max dist. selectRAM or shift reg. (bits)	24,576	8,192
Number of RAM blocks	4	4

Table 1. Resources available in XC3S50 and XC2V40.

3. The AES algorithm

The Advanced Encryption Standard (AES, Rijndael) algorithm is a symmetric block cipher that processes data block of 128, 192 and 256 bits using, respectively, keys of the same length. In this paper, only the 128 bit encryption version (AES-128) is considered. The 128-bit data block and key are considered as a byte array, respectively called *State* and *RoundKey*, with four rows and four columns.

Let a 128-bit data block in the i^{th} round be defined as:

$$data_block^i = d_{15}^i | d_{14}^i | d_{13}^i | d_{12}^i | d_{11}^i | d_{10}^i | d_9^i | d_8^i | d_7^i | d_6^i | d_5^i | d_4^i | d_3^i | d_2^i | d_1^i | d_0^i$$

where d_{15}^i represents the most significant byte of the data block of the round i . The corresponding $State^i$ is:

$$State^i = \begin{bmatrix} d_{15}^i & d_{11}^i & d_7^i & d_3^i \\ d_{14}^i & d_{10}^i & d_6^i & d_2^i \\ d_{13}^i & d_9^i & d_5^i & d_1^i \\ d_{12}^i & d_8^i & d_4^i & d_0^i \end{bmatrix}$$

AES-128 consists of ten rounds. One AES encryption round includes four transformations: *SubByte*, *ShiftRow*, *MixColumn* and *AddRoundKey*. The first and last rounds differ from the other ones. Indeed there is an additional *AddRoundKey* transformation at the beginning of the first round and no *MixColumn* transformation is performed in the last round. This is done to facilitate the decryption process.

SubByte (*SB*) is a non-linear byte substitution. It operates with every byte of the *State* separately. The substitution box (S-box) is invertible and consists of two transformations:

1. Multiplicative inverse in $GF(2^8)$. The zero element is mapped to itself.

2. An affine transform over $GF(2)$.

The *SubByte* transformation applied to the *State* can be represented as follows:

$$SB(State^i) = \begin{bmatrix} SB(d_{15}^i) & SB(d_{11}^i) & SB(d_7^i) & SB(d_3^i) \\ SB(d_{14}^i) & SB(d_{10}^i) & SB(d_6^i) & SB(d_2^i) \\ SB(d_{13}^i) & SB(d_9^i) & SB(d_5^i) & SB(d_1^i) \\ SB(d_{12}^i) & SB(d_8^i) & SB(d_4^i) & SB(d_0^i) \end{bmatrix}$$

The inverse transformation is defined *InvSubByte* (*ISB*).

ShiftRow (*SR*) performs a cyclical left shift on the last three rows of the *State*. The second row is shifted of one byte, the third row is shifted of two bytes and the fourth row is shifted of three bytes. Thus, the *ShiftRow* transformation proceeds as follows:

$$SR(SB(State^i)) = \begin{bmatrix} SB(d_{15}^i) & SB(d_{11}^i) & SB(d_7^i) & SB(d_3^i) \\ SB(d_{10}^i) & SB(d_6^i) & SB(d_2^i) & SB(d_{14}^i) \\ SB(d_5^i) & SB(d_1^i) & SB(d_{13}^i) & SB(d_9^i) \\ SB(d_0^i) & SB(d_{12}^i) & SB(d_8^i) & SB(d_4^i) \end{bmatrix}$$

The inverse *ShiftRow* operation (*InvShiftRow* (*ISR*)) is trivial.

MixColumn (*MC*) operates separately on every column of the *State*. A column is considered as a polynomial over $GF(2^8)$ and multiplied modulo x^4+1 with the fixed polynomial $c(x)$:

$$c(x) = '03'x^3 + '01'x^2 + '01'x + '02'$$

As an illustration, the multiplication by $'02'$ corresponds to a multiplication by two, modulo the irreducible polynomial $m(x) = x^8 + x^4 + x^3 + x + 1$.

This can be represented as a matrix multiplication:

$$R^i = MC(SR(SB(State^i))) = \begin{bmatrix} '02' & '03' & '01' & '01' \\ '01' & '02' & '03' & '01' \\ '01' & '01' & '02' & '03' \\ '03' & '01' & '01' & '02' \end{bmatrix} \otimes \begin{bmatrix} SB(d_{15}^i) & SB(d_{11}^i) & SB(d_7^i) & SB(d_3^i) \\ SB(d_{10}^i) & SB(d_6^i) & SB(d_2^i) & SB(d_{14}^i) \\ SB(d_5^i) & SB(d_1^i) & SB(d_{13}^i) & SB(d_9^i) \\ SB(d_0^i) & SB(d_{12}^i) & SB(d_8^i) & SB(d_4^i) \end{bmatrix}$$

To achieve the inverse operation (*InvMixColumn* (*IMC*)), every column is transformed by multiplying it with a specific multiplication polynomial $d(x)$, defined by

$$d(x) = '0B'x^3 + '0D'x^2 + '09'x + '0E'$$

AddRoundKey (*AK*) performs an addition (bit-wise XOR) of the $State^i$ with the $RoundKey^i$:

$$AK(R^i) = \begin{bmatrix} R_{15}^i & R_{11}^i & R_7^i & R_3^i \\ R_{14}^i & R_{10}^i & R_6^i & R_2^i \\ R_{13}^i & R_9^i & R_5^i & R_1^i \\ R_{12}^i & R_8^i & R_4^i & R_0^i \end{bmatrix} \oplus \begin{bmatrix} rk_{15}^i & rk_{11}^i & rk_7^i & rk_3^i \\ rk_{14}^i & rk_{10}^i & rk_6^i & rk_2^i \\ rk_{13}^i & rk_9^i & rk_5^i & rk_1^i \\ rk_{12}^i & rk_8^i & rk_4^i & rk_0^i \end{bmatrix}$$

The inverse operation (*InvAddRoundKey* (*IAK*)) is trivial.

RoundKeys are calculated with the key schedule for every *AddRoundKey* transformation. In AES-128, the original cipher key is the first *RoundKey*⁰ (rk^0) used in the additional *AddRoundKey* at the beginning of the first round. *RoundKey*^{*i*}, where $0 < i \leq 10$, is calculated from the previous *RoundKey*^{*i-1*}. Let $p(j)$ ($0 \leq j \leq 3$) be the column j of the *RoundKey*^{*i-1*} and let $w(j)$ be the column j of the *RoundKey*^{*i*}. Then the new *RoundKey*^{*i*} is calculated as follows:

$$\begin{aligned} w(0) &= p(0) \oplus (Rot(Sub(p(3))) \oplus rcon^i, \\ w(1) &= p(1) \oplus w(0) \\ w(2) &= p(2) \oplus w(1) \\ w(3) &= p(3) \oplus w(2) \end{aligned}$$

Rot is a function that takes a four byte input $[a0; a1; a2; a3]$ and rotates them as $[a1; a2; a3; a0]$. The function *Sub* applies the substitution box (S-box) to four bytes. The round constant $rcon^i$ contains values $[(02')^{i-1}; 00'; 00'; 00']$.

4. Our sequential AES implementations

Some designs propose an implementation based on one complete round, and iteratively loop data through this round until the entire encryption or decryption is achieved. Only one *State*^{*i*} is processed in one cycle. These designs are suited for feedback and non-feedback modes of operation.

As mentioned in [20], the AES round offers various opportunities of parallelism. The round is composed of 16 S-boxes and four 32-bit *MixColumn* operations, working on independent data. Only *ShiftRow* needs to deal with the entire 128-bit *State*.

Based on this observation, we propose an implementation using four S-boxes and one *MixColumn* in order to compact the design. This decreases the area by a factor of four but increases the time of one round to four cycles. In practice, only the time-space tradeoff is modified. A similar approach was proposed in [20].

4.1. Implementation of ShiftRow and InvShiftRow operations

In our design, the way to access the *State*^{*i*}, for the first quarter of the round, is described in Figure 3. We read $d_{15}^i, d_{10}^i, d_5^i, d_0^i$ in parallel from the input memory, and execute *SubByte*, *MixColumn* and *AddRoundKey*. Then we write results $d_{15}^{i+1}, d_{14}^{i+1}, d_{13}^{i+1}, d_{12}^{i+1}$ to a different output memory. The second, third, and fourth quarters of the round are managed in a similar manner, depending on *ShiftRow*.

The best FPGA solution to implement such simultaneous read and write memory accesses is proposed in [20]. The solution is based on a shift register design. As described above, all calculations from the *AddRoundKey* are written into adjacent locations of the output memory in consecutive cycles. We store first $d_{15}^{i+1}, d_{14}^{i+1}, d_{13}^{i+1}, d_{12}^{i+1}$ in parallel, then $d_{11}^{i+1}, d_{10}^{i+1}, d_9^{i+1}, d_8^{i+1}$ in parallel, and so on. Therefore we can store the consecutive round results into shift registers (one shift register per row of the *State*, four shift registers for four rows). Xilinx FPGAs propose a very space efficient solution to achieve a 16-bit shift register with a dynamic variable access. Four slices can implement an 8-bit wide, 16-bit long shift register. The four dynamic variable accesses are used to read the input memory content at correct positions into the rows. Four 8-bit wide shift register are needed, which corresponds to 16 slices.

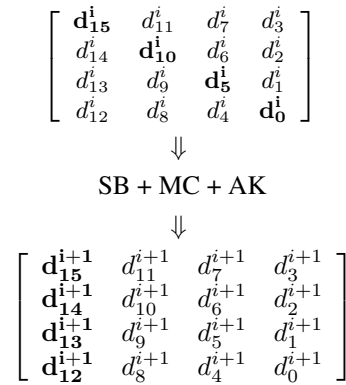


Figure 3. Memory accesses involved in the first calculation step of the round *i*.

The *InvShiftRow* operation can be done using the same shift registers modifying the way to access the input memory.

4.2. Implementation of SubByte/MixColumn and InvSubByte/InvMixColumn

Compared to the paper [20], we propose a more efficient combination of *SubByte* and *MixColumn* operations, i.e. we use less resources than separated block implementations. Our solution takes advantage of specific features of the new Xilinx devices and perfectly fits into the Spartan-3 or Virtex-II technologies⁴.

The Spartan-3 and Virtex-II FPGAs have both dedicated 18-Kbit dual-port RAM blocks⁵, that can be used to store tables for the combination of *SubByte* and *MixColumn*.

As also mentioned in [4], the consecutive *SubByte* and *MixColumn* operations on the first quarter of the round can be expressed as $e_{15..12}^i$:

$$\begin{bmatrix} e_{15}^i \\ e_{14}^i \\ e_{13}^i \\ e_{12}^i \end{bmatrix} = \begin{bmatrix} '02' & '03' & '01' & '01' \\ '01' & '02' & '03' & '01' \\ '01' & '01' & '02' & '03' \\ '03' & '01' & '01' & '02' \end{bmatrix} \otimes \begin{bmatrix} SB(d_{15}^i) \\ SB(d_{10}^i) \\ SB(d_5^i) \\ SB(d_0^i) \end{bmatrix}$$

which is also equivalent to:

$$\begin{bmatrix} '02' \\ '01' \\ '01' \\ '03' \end{bmatrix} \otimes [SB(d_{15}^i)] \oplus \begin{bmatrix} '03' \\ '02' \\ '01' \\ '01' \end{bmatrix} \otimes [SB(d_{10}^i)] \oplus \begin{bmatrix} '01' \\ '03' \\ '02' \\ '01' \end{bmatrix} \otimes [SB(d_5^i)] \oplus \begin{bmatrix} '01' \\ '01' \\ '03' \\ '02' \end{bmatrix} \otimes [SB(d_0^i)]$$

If we define four tables (T_0 to T_3) with 256 4-byte data as:

$$\begin{aligned} T_0(a) &= \begin{bmatrix} '02' \bullet SB(a) \\ SB(a) \\ SB(a) \\ '03' \bullet SB(a) \end{bmatrix} \\ T_1(a) &= \begin{bmatrix} '03' \bullet SB(a) \\ '02' \bullet SB(a) \\ SB(a) \\ SB(a) \end{bmatrix} \\ T_2(a) &= \begin{bmatrix} SB(a) \\ '03' \bullet SB(a) \\ '02' \bullet SB(a) \\ SB(a) \end{bmatrix} \end{aligned}$$

⁴It is not the case with Spartan-II.

⁵The Spartan-II has dedicated 4-Kbit dual-port RAM blocks.

$$T_3(a) = \begin{bmatrix} SB(a) \\ SB(a) \\ '03' \bullet SB(a) \\ '02' \bullet SB(a) \end{bmatrix}$$

The combination of *SubByte* followed by *MixColumn* can be expressed as:

$$\begin{bmatrix} e_{15}^i \\ e_{14}^i \\ e_{13}^i \\ e_{12}^i \end{bmatrix} = T_0(d_{15}^i) \oplus T_0(d_{10}^i) \oplus T_0(d_5^i) \oplus T_0(d_0^i)$$

The size of one T_i table is 8 Kbits for encryption. The corresponding similar table for decryption also takes 8 Kbits (IT_0 to IT_3). It is therefore possible to achieve the complete *SubByte/MixColumn* and *InvSubByte/InvMicolumn* operations using two dual-port 18-Kbit RAM blocks.

The proposed solution significantly reduces the resources used in [20].

4.3. Encryption/Decryption design choices

One of the inconveniences of AES comes from the fact that the *AddRoundKey* is executed after *MixColumn* in the case of encryption and before *InvMixColumn* in the case of decryption. Such encryption/decryption implementation will therefore require additional switching logic to select appropriate data paths, which can also affects the time performance. The paper [20] mentions this problem but chooses to design like that anyway.

AES decryption algorithm nevertheless allows *InvMixColumn* and *AddRoundKey* to be re-ordered if we perform an additional *InvMixColumn* operation on most of the *RoundKeys* (except the first and the last *RoundKeys*). More details about such scheduling of operations can be found in [4, 5]. At first sight, *InvMixColumn* could seem to require much more area than the switching logic. This is especially true if the *InvMixColumn* of the round is narrowly combined with the *InvSubByte* in RAM blocks. Nevertheless, the subsection 4.4 proposes a solution using very few additional resources but some extra cycles to generate all inverse *Roundkeys* (*InvRoundKeys*). Figure 4 summarizes our design choices concerning the data path round.

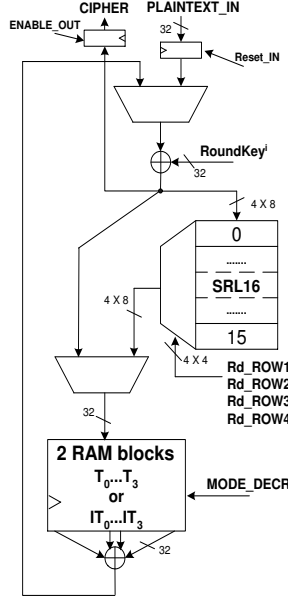


Figure 4. Our AES data path round.

4.4. Implementation of the key schedule

The implementation of our AES key schedule is based on precomputing *RoundKeys* and *InvRoundKey* in advance and storing them in one RAM block. The difficult computation of the *InvRoundkeys* on-the-fly⁶ completely justifies this approach.

Our implementation of the key schedule is shown in Figure 5. First, it computes 32-bits of all the *RoundKey*ⁱ per clock cycle. The results are stored in one dual-port block RAM, thanks to the first port. This step takes 44 clock cycles. In the same time, we also store *SB(RoundKeys)* data in the same RAM, but using the other port. It corresponds to the first step of the calculation process of *InvRoundKeys*. As mentioned in the subsection 4.3, *InvRoundKey*ⁱ equals to *IMC(RoundKey*¹⁰⁻ⁱ), except for the first *InvRoundKey*⁰ and last *InvRoundKey*¹⁰, which equal to respectively *RoundKey*¹⁰ and *RoundKey*⁰.

If we need decryption processes, a second step has to be applied to *SB(RoundKeys)*. Therefore, we start to calculate *ISB(SB(RoundKey*¹⁰)) and store it as *InvRoundKey*⁰. Then, we evaluate the result *IMC(ISB(SB(RoundKey*¹⁰⁻ⁱ))) which equals to *IMC(RoundKey*¹⁰⁻ⁱ) and we store it as *InvRoundKey*^{1..9}. *InvRoundKey*¹⁰ is generated as *InvRoundKey*⁰. This optional decryp-

⁶It is a real weak aspect of AES algorithm.

tion process takes 48 cycles to generate the complete *InvRoundKeys*.

Due to *InvRoundKey*⁰ and *InvRoundKey*¹⁰, tables (*T*₀ to *T*₃) need to be changed. *InvSubByte* has to replace the duplicated *SubByte*. We define new 16-Kbit tables (*CT*₀ to *CT*₃) combined with (*IT*₀ to *IT*₃). *CT*₀ is illustrated below as an example:

$$CT_0(a) = \begin{bmatrix} '02' \bullet SB(a) & '0E' \bullet SB(a) \\ SB(a) & '09' \bullet SB(a) \\ ISB(a) & '0D' \bullet SB(a) \\ '03' \bullet SB(a) & '0B' \bullet SB(a) \end{bmatrix}$$

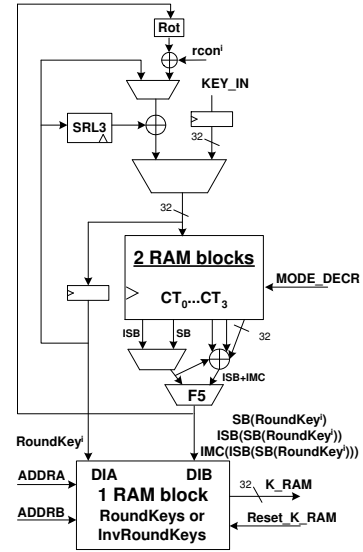


Figure 5. Our AES key schedule.

4.5. Implementation and results of our complete AES

Our final AES design combines the data path part and the key schedule part. Since the key schedule is done with precomputation, this part does not work simultaneously with the encryption/decryption process. It is therefore possible to share resources between both circuits. Both parts of the circuit were thought to perfectly fuse together without additional slices⁷ and tri-state buffers. This allows reaching higher frequency than in [20]. The global design is shown in Figure 6. We fused the key and plaintext inputs to one register. The input and output registers are packed into IOBs to improve the resources used and the global frequency of the design.

⁷Only new F5 multiplexers are required.

Algo.	Gaj's AES	Ours AES	Ours AES	Ours DES	Ours 3-DES
Device	XC2S30-6	XC3S50-4	XC2V40-6	XC2V40-6	XC2V40-6
Slices	222	163	146	189	227
Through. (Mbps)	166	208	358	974	326
RAM blocks	3	3	3	0	0
Throughput/Area (Mbps/slices)	0.75	1.26	2.45	5.15	1.44

Table 2. Comparisons with other sequential block cipher implementations.

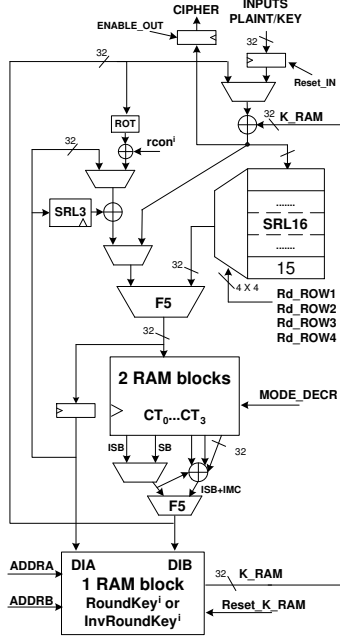


Figure 6. Our complete AES design.

The synthesis of our complete design was done using Synplify Pro 7.2 from Synplicity. The place and route were done using Xilinx ISE 6.1.02i package. The final results are given in Table 3 for Spartan-3 and Virtex-II.

As a comparison, we also set up a table with the previous AES [20], DES and 3-DES [16] results. Table 2 shows the results of these compact encryption/decryption circuits. Like others papers, we also define a ratio $Throughput/Area$ to facilitate comparisons. We finally achieve an implementation of AES which is 68% better in terms of $Throughput/Area$ assuming that Spartan-II and Spartan-3 are equivalent.

In comparison with the most efficient compact 3-DES circuits in XC2V40-6, we can conclude that AES is more effective if we do not care about the use

Device	XC3S50-4	XC2V40-6
LUTs used	293	288
Registers used	126	113
Slices used	163	146
RAM blocks	3	3
Latency (cycles)	46	46
Out. every (cycles)	1/44	1/44
Frequency	71.5 MHz	123 MHz

Table 3. Final results of our complete sequential AES.

of three internal RAM blocks. However, 3-DES remains interesting for applications that need to regularly change the key for encryption or decryption. Indeed, our AES design takes 92 cycles, in the worst case, to calculate a new complete *InvRoundKeys*.

5. Conclusion

In this paper, we propose solutions for a very compact and effective FPGA implementation of the AES. We combine narrowly the non-linear S-boxes and the linear diffusion layer thanks to specific features of recent Xilinx devices. We also propose a low-cost solution to deal with the subkeys computed during the decryption step. In addition, we merge efficiently the key schedule and the data path parts.

The resulting implementations fits in a very inexpensive Xilinx Spartan-3 XC3S50 FPGA, for which the cost starts below \$10 per unit. This implementation can encrypt and decrypt a throughput up to 208 Mbps, using 163 slices. The design also fits in Xilinx Virtex-II XC2V40 and produces data streams up to 358 Mbps, using 146 slices. In comparison with 3-DES, AES is more efficient if we do not care about the use of three internal FPGA RAM blocks.

The throughput, low-cost and flexibility of our solution make it perfectly practical for cryptographic em-

bedded applications.

References

- [1] J.M. Rabaey. *Digital Integrated Circuits*. Prentice Hall, 1996.
- [2] Xilinx. The Virtex-II field programmable gate arrays data sheet, available from <http://www.xilinx.com>.
- [3] National Bureau of Standards. *FIPS PUB 46*, The Data Encryption Standard. U.S. Department of Commerce, Jan 1977.
- [4] J. Daemen and V. Rijmen. The Block Cipher RIJNDael, NIST's AES home page, available from <http://www.nist.gov/aes>.
- [5] P.Baretto, V.Rijmen, *The KHAZAD Legacy-Level Block Cipher*, Submission to NESSIE project, available from <http://www.cosic.esat.kuleuven.ac.be/nessie/>
- [6] S. Trimberger, R. Pang and A. Singh. A 12 Gbps DES encryptor/decryptor core in an FPGA. In *Proc. of CHES'00*, LNCS, pages 156–163. Springer, 2000.
- [7] Xilinx, V. Pasham and S. Trimberger. High-Speed DES and Triple DES Encryptor/Decryptor. available from <http://www.xilinx.com/xapp/xapp270.pdf>, Aug 2001.
- [8] Helion Technology. High Performance DES and Triple-DES Core for XILINX FPGA. available from <http://www.heliontech.com>.
- [9] CAST, Inc. Triple DES Encryption Core. available from <http://www.cast-inc.com>.
- [10] CAST, Inc. DES Encryption Core. available from <http://www.cast-inc.com>.
- [11] inSilicon. X3 DES Triple DES Cryptoprocessor. available from <http://www.insilicon.com>.
- [12] inSilicon. X_DES Cryptoprocessor. available from <http://www.insilicon.com>.
- [13] P. Chodowicz, K. Gaj, P. Bellows and B. Schott. Experimental Testing of the Gigabit IPsec-Compliant Implementations of RIJNDael and Triple DES Using SLAAC-IV FPGA Accelerator Board. In *Proc. of ISC 2001: Information Security Workshop*, LNCS 2200, pp.220-234, Springer-Verlag.
- [14] J.P. Kaps and C. Paar. Fast DES Implementations for FPGAs and Its Application to a Universal Key-Search Machine. In *Proc. of SAC'98: Selected Areas in Cryptography*, LNCS 1556, pp. 234-247, Springer-Verlag.
- [15] G. Rouvroy, FX. Standaert, JJ. Quisquater, JD. Legat. Efficient Uses of FPGA's for Implementations of DES and its Experimental Linear Cryptanalysis. In *IEEE Transactions on Computers*, Special CHES Edition, pp. 473-482, April 2003.
- [16] G. Rouvroy, FX. Standaert, JJ. Quisquater, JD. Legat. Design Strategies and Modified Descriptions to Optimize Cipher FPGA Implementations: Fast and Compact Results for DES and TripleDES. In the proceedings of FPL 2003, Lecture Notes in Computer Science, vol 2778, pp. 181-193, Springer-Verlag.
- [17] FX. Standaert, G. Rouvroy, JJ. Quisquater, JD. Legat. A Methodology to Implement Block Ciphers in Reconfigurable Hardware and its Application to Fast and Compact AES Rijndael. In the proceedings of FPGA 2003, pp. 216-224, ACM.
- [18] FX. Standaert, G. Rouvroy, JJ. Quisquater, JD. Legat. Efficient Implementation of Rijndael Encryption in Reconfigurable Hardware: Improvements and Design Tradeoffs. In the proceedings of CHES 2003, Lecture Notes in Computer Science, vol 2779, pp. 334-350, Springer-Verlag.
- [19] P. Chodowicz and K. Gaj. Comparison of the Hardware Performance of the AES Candidates using Reconfigurable Hardware. The Third Advanced Encryption Standard (AES3) Candidate Conference, April 13-14 2000, New York, USA.
- [20] K. Gaj and P. Chodowicz. Very Compact FPGA Implementation of the AES Algorithm. In the proceedings of CHES 2003, Lecture Notes in Computer Science, vol 2779, pp. 319-333, Springer-Verlag.
- [21] V. Fischer and M. Drutarovsky. Two Methods of RIJNDael Implementation in Reconfigurable Hardware. In the proceedings of CHES 2001: The Third International CHES Workshop, Lecture Notes In Computer Science, LNCS2162, pp 65-76, Springer-Verlag.
- [22] A. Rudra et al. Efficient RIJNDael Encryption Implementation with Composite Field Arithmetic. In the proceedings of CHES 2001: The Third International CHES Workshop, Lecture Notes In Computer Science, LNCS2162, pp 65-76, Springer-Verlag.
- [23] M. McLoone and J.V. McCanny, High Performance Single Chip FPGA RIJNDael Algorithm Implementations. In the proceedings of CHES 2001: The Third International CHES Workshop, Lecture Notes In Computer Science, LNCS2162, pp 65-76, Springer-Verlag.
- [24] M. McLoone and J.V. McCanny, Single-Chip FPGA Implementation of the Advanced Encryption Standard Algorithm. In the proceedings of FPL 2002: The Field Programmable Logic Conference, Lecture Notes in Computer Science, LNCS 2147, p.152ff.
- [25] K.U. Jarvinen, M.T. Tommiska and J.O. Skytta A fully Pipelined Memoryless 17.8 Gbps AES-128 Encryptor. In the proceedings of FPGA 2003: Symposium on Field-Programmable Gate Arrays, pp. 207-215, ACM.
- [26] N. Weaver and J. Wawrzyniek. High Performance Compact AES Implementations in Xilinx FPGAs. available from <http://www.cs.berkeley.edu/~nweaver/Rijndael..>